

## Geomagnetic anomalies recorded in L9 of the Songjiadian loess section in southeastern Chinese Loess Plateau

WANG DaoJing<sup>1\*</sup>, WANG YongCheng<sup>2</sup>, HAN JingTai<sup>1</sup>, DUAN MuGang<sup>3</sup>, SHAN JiaZeng<sup>1</sup> & LIU TungSheng<sup>1</sup>

<sup>1</sup>Key Laboratory of Cenozoic Geology and Environment, Institute of Geology and Geophysics, Chinese Academy of Sciences, Beijing 100029, China;

<sup>2</sup>China University of Geosciences, Beijing 100083, China;

<sup>3</sup>School of Information Science and Technology, Beijing Institute of Technology, Beijing 100081, China

Received May 20, 2009; accepted July 23, 2009; published online October 30, 2009

Detailed magnetostratigraphic and rock magnetic investigations on L8–S12 of the Songjiadian loess section in the Sanmenxia area, southernmost margin of the Chinese Loess Plateau were conducted in this study. Matuyama/Brunhes (M/B) boundary occurred at the bottom of the loess unit L8. The top and bottom boundaries of the Jaramillo polarity subchron are found in the middle of L10 and the bottom of L12, respectively. Magnetic fabric of the loess layers maintains the original depositional features and the recorded remanent magnetization analysis indicates little post-deposition disturbance experienced. In late Matuyama chron, two anomalies of geomagnetic field have been detected in L9. Our data demonstrated that these recorded anomalies were less likely a result of remagnetization, but more possibly the signature of geomagnetic excursions occurred, named SJD1 and SJD2. It is calculated that the midpoint ages of SJD1 and SJD2 are 0.917 Ma and 0.875 Ma, respectively, and the time-interval between the two events approximates 12 ka. Chronologically, SJD1 is close to the Santa Rosa (0.922 Ma) and SJD2 corresponds to the Kamikatsura (0.886 Ma) excursions. In consistence with previous studies, the geomagnetic field was weakened during these events.

**Paleomagnetism, polarity event, loess, Sanmenxia**

**Citation:** Wang D J, Wang Y C, Han J T, et al. Geomagnetic anomalies recorded in L9 of the Songjiadian loess section in southeastern Chinese Loess Plateau. Chinese Sci Bull, 2010, 55: 520–529, doi: 10.1007/s11434-009-0565-9

Geomagnetic polarity reversal is one of the most basic and important characteristics of geomagnetic field. Studying the spatial and temporal variation characteristics of geomagnetic field during polarity conversion helps us deepen understanding on the mechanism of geomagnetic polarity reversal and its evolutionary history. Geomagnetic excursion as a short polarity event has a close relation with geodynamo of earth's outer core [1], but due to the shortage of reliable data, its detailed operating mechanism still needs further researching. In recent twenty years, following the acquisition of massive high-resolution geomagnetic data from the deep ocean sediment, people came to know the high frequency of geomagnetic excursion and its global significance. Up till present, it has been found many times

from marine sediment that short polarity event of geomagnetic field occurred in the period of 0.78–0.99 Ma [2–4]. The same is true of lava research. When doell et al.[5] studied Cerro Santa Rosa I dome lava in New Mexico in 1966, they discovered Santa Rosa normal polarity event in the first time. The follow-up studies gave  $^{40}\text{Ar}/^{39}\text{Ar}$  age data of 0.92–0.936 Ma [6,7]. When Maenaka [8] studied the Osaka Formation Kamikatsura tuff in the southwest of Japan in 1983, he confirmed and named Kamikatsura normal polarity event in the first time. The numerous follow-up studies gave the K-Ar or  $^{40}\text{Ar}/^{39}\text{Ar}$  age of this event in different areas. It is 0.821–0.900 Ma [9–12]. The ODP 983/984 borehole data indicate the Kamikatsura event and the Santa Rosa event correspond to Marine Isotope Stage MIS 21 and MIS 25top [13–15], respectively.

\*Corresponding author (email: djwang@mail.iggcas.ac.cn)

Chinese loess-paleosol sequences are good media for the research on the paleoclimatic changes [16–25] since 2.5 Ma and the long-term changes of geomagnetic field. Meanwhile, magnetostratigraphic research also has effectively established the chronological framework of loess-paleosol sequences. Some scholars questioned the existence of the remarkable Lock-in and Smoothing effects in loess and paleosol as well as the authenticity and accuracy of the geomagnetic field information recorded in them [26,27], but recent research finding indicates the remanent magnetization of the loess at some horizons (for example: L1 in Lingtai, Shaanxi Province) does not have much Smoothing effect during the lock-in process, and it can record the long-term changes of geomagnetic field with an accurate time resolution [28,29]. During the 1980s–1990s, some scholars discovered normal polarity event existed in loess unit L9 in different areas of the Chinese Loess Plateau (CLP) [30–33], but the research was not continued and deepened due to the limitation of epistemic and testing means as well as the absence of synchronous lava and marine geomagnetic chronological data. Recently, Yang et al. [34] discovered two short polarity events in L9 at Baoji. As the age data they obtained are close to the Kamikatsura and Santa Rosa  $^{40}\text{Ar}/^{39}\text{Ar}$  age data, these events were confirmed as two excursions. However, the finding of the research made by Wang et al. [35] on L9 in Sha'anxian, Henan Province gives another view and thinks the normal polarity indication in L9 is the remagnetization phenomenon controlled by lithology other than the record of geomagnetic excursion. Therefore, in order to find out the real geomagnetic field information recorded in L9, further research is very necessary.

Through analyzing the pedogenesis, remanent magnetization characteristics, accumulation rate and magnetic fabric of the L8–S12 of Songjiadian loess section (34.7°N, 111.3°E) in Sanmenxia, this article made further research on whether the loess unit L9 records Kamikatsura and Santa Rosa geomagnetic excursions between M/B–UJ/M in late Matuyama chron.

## 1 Researched section and sampling

The Songjiadian loess section is located in the Sanmenxia area, southeastern CLP, adjacent to a loess platform on the southern bank of the Yellow River. The loess-paleosol sequences crop out completely. Spatially, it is spread horizontally with a thickness of about 124 m. The underlying red clay is about 7 m thick and unconformably overlying a gravel layer. The L9 in this section, which was deposited during a glacial period under arid and cold conditions [36], is characterized by large thickness (up to 11 m), high deposition rate, coarse grain size (Figure 5) and weak pedogenesis. This study focuses on the loess-paleosol sequence from top of L8 to the bottom of S12 covers a thickness of 25.9 m. Two parallel sets of oriented paleomagnetic specimens were

continuously collected with a size of 8 cm×8 cm×8 cm in the field, processed into 2 cm×2 cm×2 cm cubic in the lab (at least 4 samples at each horizon), and used for rock magnetism and the remanent magnetization analyses.

## 2 Rock magnetic experiments

The analysis on the types and content of the magnetic minerals contained in paleomagnetic samples is an important basis for the judgment on the reliability of the obtained paleomagnetic data. Saturation isothermal remanent magnetization (SIRM) is an important parameter to identify the types and grain size of magnetic minerals. Acquisition curves of isothermal remanent magnetization (IRM) in stepwise increasing fields up to 2.7 T indicate that 90% of the SIRM is acquired below 350 mT for both loess and paleosol specimens (Figure 1), which suggests that low-coercivity magnetic carriers (magnetite and/or maghemite) are dominant in the studied sediments. The IRM acquisition curves also show a continuous increase up to an applied field of 2.7 T in which the saturation is not fully reached, which also indicates the presence of high-coercivity magnetic carriers (goethite and/or hematite).

The result of the thermal demagnetization of a three-axis IRM reveals (Figure 2): The unblocking temperature of low-coercivity component (<0.15 T) is 580°C, which tallies with the characteristic of magnetite, and the unblocking temperature of high-coercivity component (0.4–2.7 T) is 680°C, which suggests the existence of hematite. The curve of medium-coercivity component (0.15–0.4 T) has an inflexion at about 300°C, which implies the possible existence of maghemite. The above information indicates the samples from different depths of L9 do not have material difference in magnetic carrying minerals, and the magnetic minerals are mostly magnetite and may also contain a certain amount

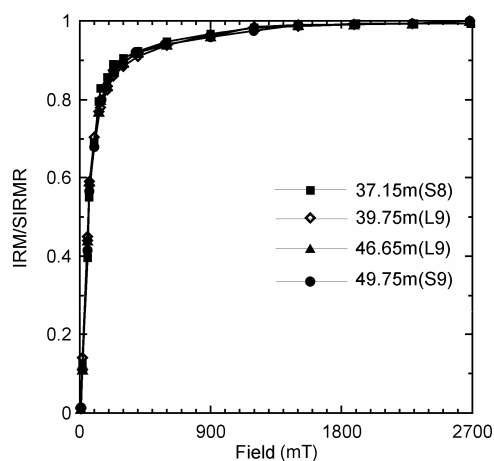


**Figure 1** Stepwise acquisition of isothermal remanent magnetization (IRM)/saturation isothermal remanent magnetization (SIRM) in progressively increasing fields up to 2.7 T for loess/paleosol (S8–L9) samples of the Songjiadian section.

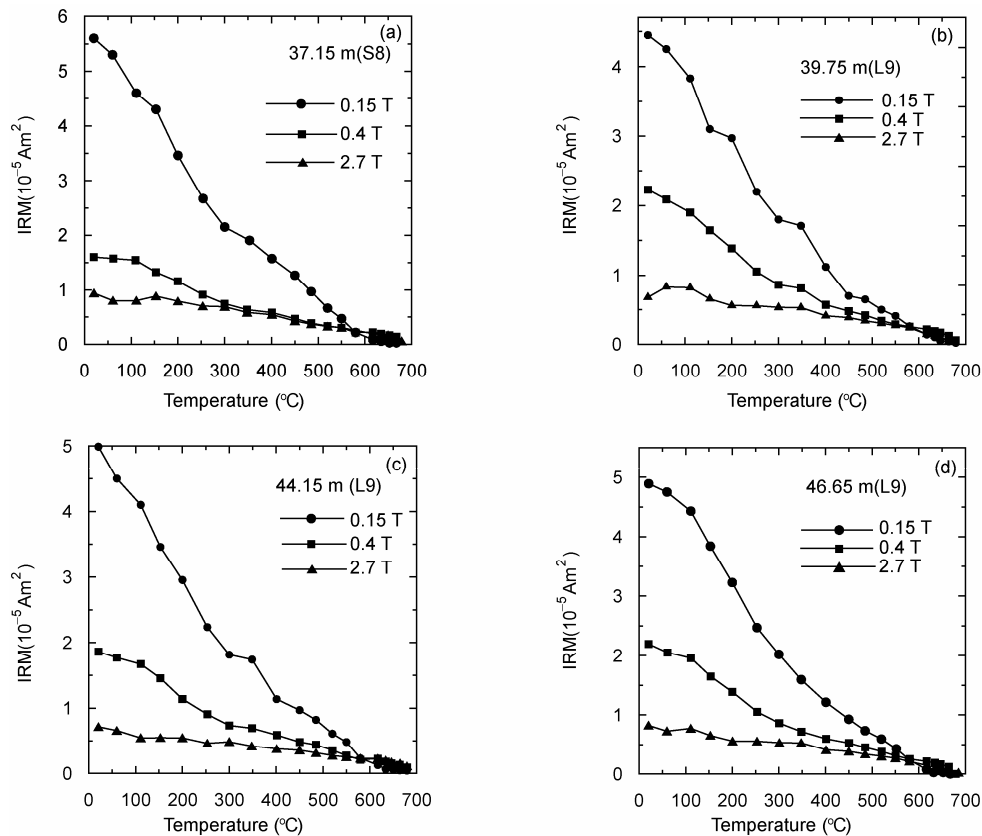


**Figure 2** Thermal demagnetization of a three-component IRM for loess/paleosol samples of the Songjiadian section. The sample in Figure 2(a) is from unit S8, the others are from unit L9.

of maghemite, hematite and goethite. However, as the L9 of this section is very thick, there might be proximal source substances. The result of thermal demagnetization also shows the existence of secondary goethite (see Figure 6(c), (d)). Therefore, it is believed that the rock magnetic characteristics of the L9 in the Songjiadian section bear resemblance with the loess in the hinterland of the CLP [30–33] and at the same time, it also has its own features.

The analysis on the magnetic fabric of the samples from S8, L9 and L15 indicates (Figure 3) foliation ( $F$ ) is basically consistent with horizontal plane. On this section, degree of anisotropy ( $P$ ), shape factor ( $T$ ) and other parameters of AMS ellipsoid do not have much variation. With the increase of depth,  $F$  increases slightly. This should be caused by compaction. The inclinations of the susceptibility maximum axes ( $\text{Inc-}K_{\text{max}}$ ) of the samples in the whole L9 as well as the S8 above it and the L15 below it all show the characteristics of the normal depositional magnetic fabric usually below  $20^\circ$  (Figure 4), because according to other people's research [37,38], the anisotropy of magnetic susceptibility of eolian loess in the CLP is mainly caused by foliation which is parallel with the depositional horizon; the minimum susceptibility axes  $K_{\text{min}}$  is perpendicular to depositional horizon. This suggests the magnetic fabric in Songjiadian section maintains the characteristics of original de-

posit fabric and the recorded remanent magnetization should not have met with obvious post-deposition disturbance [37]. From Figure 3, we can see that the  $\text{Dec-}K_{\text{max}}$  in a cold period is mainly distributed along SN direction, most likely reflecting that the magnetic grains were transported principally by northwesterly or northerly winds. A slight but discernable difference in the dominant direction between the paleosol (S8) and loess (L9) samples is possibly attributable to pedogenic modification.

From the grain size curves of L8–S12 of the Songjiadian section, it can be seen that both median grain-size ( $Md$ ) and the component of  $<2 \mu\text{m}$ ,  $>63 \mu\text{m}$  change regularly with the alternation of cold period and warm period (see Figure 5).  $Md$  is usually regarded as an indicator of wind strength [39]. The clay component of  $<2 \mu\text{m}$  may indicate the degree of pedogenesis. The fine sand component of  $>63 \mu\text{m}$  can hardly be suspended and transported [40], so it is usually regarded as an indicator of dust source zone and height of transporting wind. In the periods corresponding to L9, the clay component of  $<2 \mu\text{m}$  has a small peak at around 45.7 m, but its average content is below 10% and low in the whole section. This indicates its pedogenesis is very weak. In comparison,  $Md$  ( $-20 \mu\text{m}$  on average) and the component of  $>63 \mu\text{m}$  ( $-12\%$  on average) show relatively high value in the whole section, and the content of the

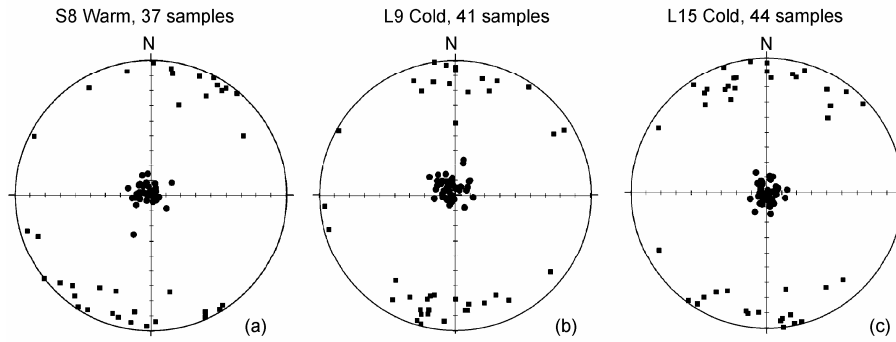


**Figure 3** Results of AMS principal directions for the samples of Songjiadian section corresponding to (a) warm and (b), (c) cold periods. Squares and circles represent directions of the maximum and minimum susceptibility, respectively.

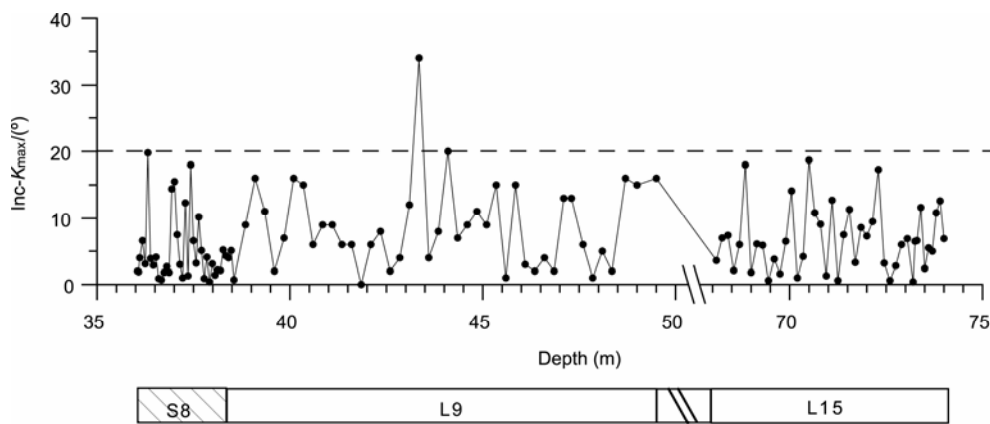


**Figure 4** Depth plots of  $Inc-K_{max}$ .

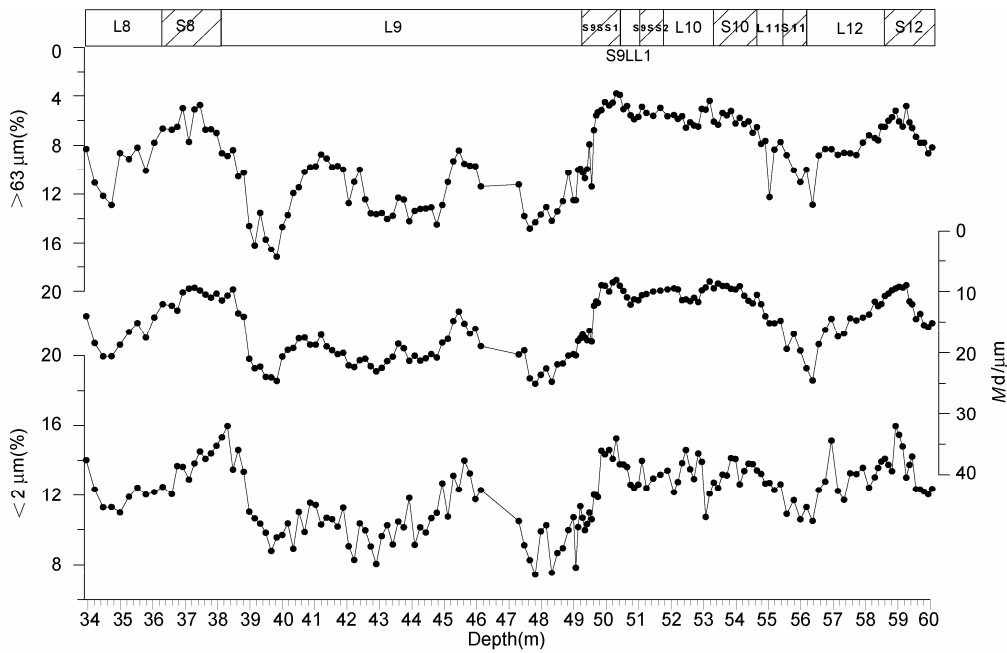


**Figure 5** Stratigraphy and grain size distribution (L8–S12) of the Songjiadian section.

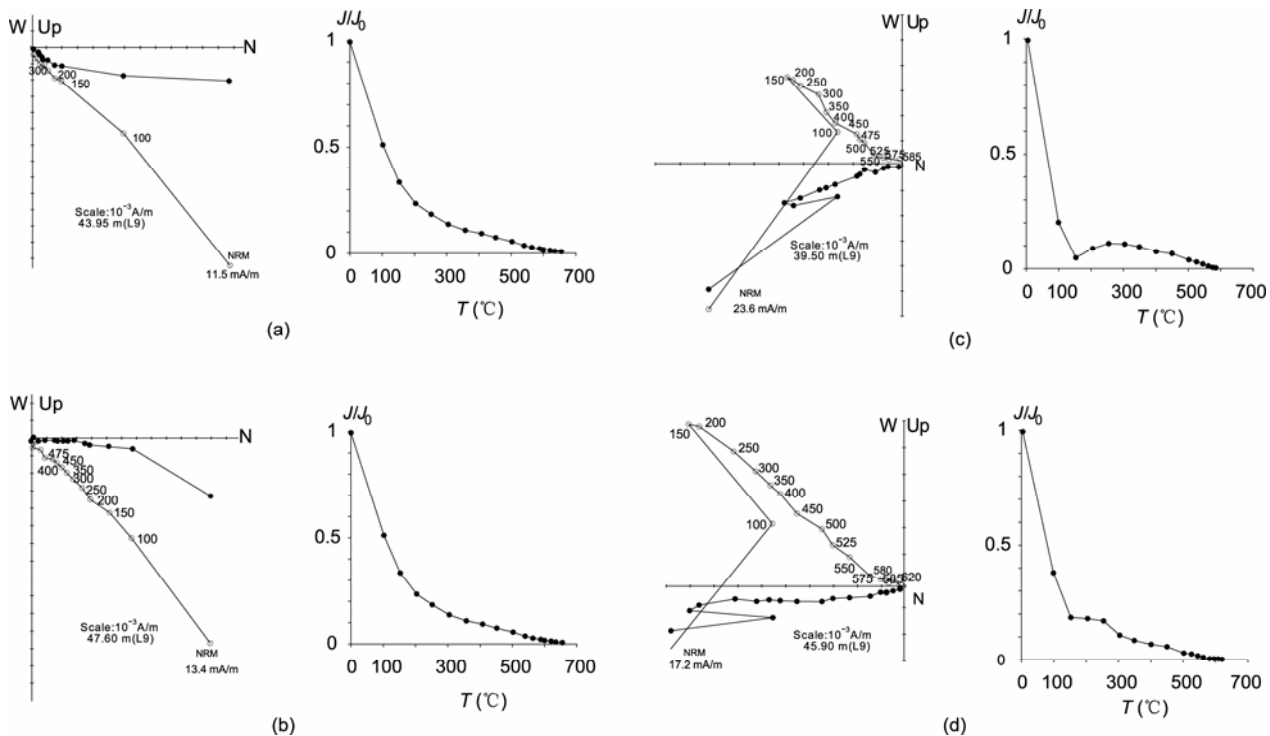


**Figure 6** Orthogonal demagnetization diagrams (left) and normalized intensity decay plots (right) showing typical thermal demagnetization behaviors of the studied samples from L9 of Songjiadian section. Solid (open) symbols represent the projections onto the horizontal (vertical) plane. Number indicates the heating temperature.

component of  $> 63 \mu\text{m}$  is even higher than that in central north of Loess Plateau[41], indicating the dust transporting wind becomes stronger and some proximal source coarse grain are carried, too. It is probably the fundamental reason why the L9 in Songjiadian section is very thick.

### 3 Paleomagnetic results

The low-field magnetic susceptibility was measured for all specimens using a Bartington MS2 magnetic susceptibility meter. All samples were subjected to thermal demagnetization. The remanent magnetization was measured with 2G vertical cryogenic magnetometer inside a field-free space ( $< 300 \text{ nT}$ ), at the Paleomagnetism Laboratory of the Institute of Geology and Geophysics, Chinese Academy of Sciences. Stepwise thermal demagnetization of the natural remanent magnetization (NRM) was carried out on every sample, up to  $585^\circ\text{C}$  at  $10\text{--}50^\circ\text{C}$  intervals. The result indicates the NRM direction of the samples is basically consistent with present-day geomagnetic field direction, some samples have a single remanent magnetization component (Figure 6(a), (b)) and in some demagnetized samples (Figure 6(c), (d)) remanent magnetization component with two temperature ranges ( $0\text{--}100$  ( $200$ ) $^\circ\text{C}$  and  $200\text{--}580^\circ\text{C}$ ) can be separated. In the latter, stable ChRM directions were determined after  $200\text{--}300^\circ\text{C}$  and decays toward the origin of the vector component diagram. The NRM intensity of some

samples declines obviously at  $100\text{--}150^\circ\text{C}$  (Figure 6(c), right). In combination with the above result of thermal demagnetization of the three-axis IRM, we think that the ChRM component is mainly carried by magnetite. In order to further verify the reliability of experimental result, we did stepwise thermal demagnetization experiment on the two groups of parallel samples collected from a same sampling plane and determined ChRM through principal component analysis. The experimental results of the two groups of parallel samples have good consistency. This implies that the paleomagnetic record obtained is reliable.

According to the ChRM direction and virtual geomagnetic pole (VGP) latitudes of the sample points in the stratum (Figure 7), it is clear that M-B boundary occurred at the bottom of L8, UJ-M boundary is at the middle of L10 and J-M boundary is at the bottom of L12. This result tallies with the previous studies [42]. In L9, two anomalies of geomagnetism are recorded at the depth of  $42.25\text{--}45.15 \text{ m}$  and  $46.10\text{--}48.00 \text{ m}$ , respectively. For the authenticity of paleomagnetic anomaly conform to the following hypotheses [28]: (1) no obvious evidence for local hiatus, deformation (such as tilting, wedging, and involution) based on direct field observations; (2) direct orientation of block samples at the sampling site and careful preparation of sub-samples in the laboratory; (3) normal AMS or lacking of correlation between  $\text{Inc}$  and  $\text{Inc-K}_{\text{max}}$ ; and (4) well defined ChRM. Therefore, we may think the anomalies reflect the changes of geomagnetic field. However, considering

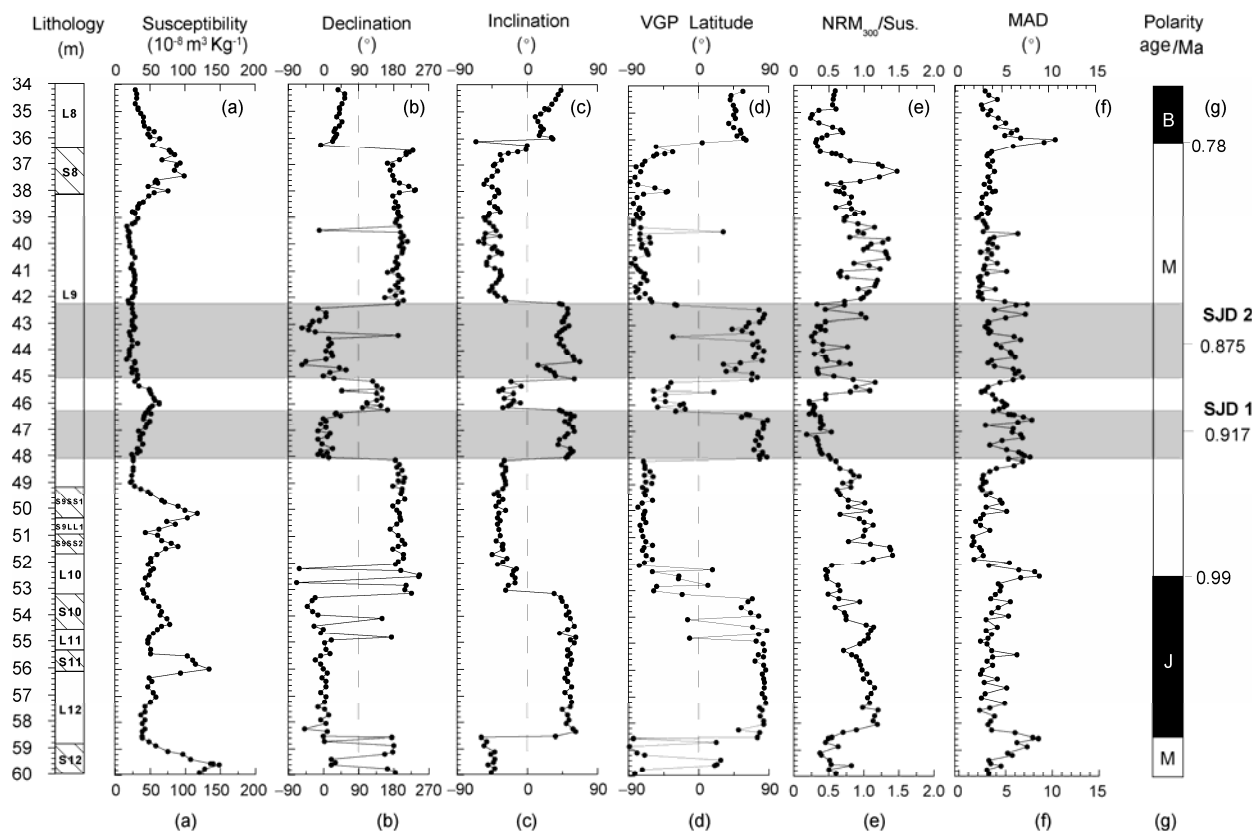


**Figure 7** Magnetic results for the Songjiadian section. (a) Low-field magnetic susceptibility; (b) declination and (c) inclination of the ChRM; (d) virtual geomagnetic pole (VGP); (e)  $NRM_{300}$ /susceptibility as a proxy for relative paleointensity variations; (f) maximum angular deviation (MAD) values and (g) magnetic polarity (black (white) = normal (reverse) polarity; grey = excursions). Polarity boundary ages are after Cande and Kent (1995) [60]. B represents the Brunhes Chron, M represents the Matuyama Chron, and J represents the Jaramillo Subchron.

that the reason for the anomalies of remanent magnetization is not fully identified and there is the possibility of remagnetization, we named the above anomalies of remanent magnetization SJD 1 and SJD 2 (the grey zones in Figure 7) for the time being. The data of the high-resolution relative paleointensity from deep-ocean boreholes demonstrate the intensity of geomagnetic field shows a trend of sharp decrease during geomagnetic polarity reversal and geomagnetic excursions [43,44]. The research on the geomagnetic polarity reversal recorded in loess also verifies the above result [45,46]. As magnetic minerals and the grain size of sediment with high uniformity are suitable for relative paleointensity studies [47,48], and the magnetic uniformity of loess unit L9 which perfectly records the two anomalies of remanent magnetization conforms to these characteristics (Figures 1 and 2), in this research we have tentatively selected  $NRM_{300}$  normalized by the low-field magnetic susceptibility as the proxy for the relative paleointensity variation (Figure 7(e)). It is evident that a marked paleointensity minimum occurred during the period correspond to both two sections with anomaly of remanent magnetization, B/M boundary and M/J boundary. The way of intensity change is gradual change. The interval between the two sections with abnormal remanent magnetization exhibits a clear rise in

relative paleointensity

#### 4 Discussion on the cause of abnormal geomagnetic record

Some geomagnetic excursions have been discovered and confirmed in Chinese loess-paleosol sequences [25, 28, 29, 34, 47, 49–54]. The periods involved are mostly in Brunhes and mid/late Matuyama, but more researches were done on Mono Lake, Laschamp, Black and other geomagnetic excursions recorded in the loess stratum of late Brunhes [22, 25, 28, 47, 51]. This is because on the one hand, the magnetic susceptibility and grain size indicator of the loess stratum in the last glacial stage and interglacial stage can be clearly compared with and differentiated from oxygen isotope stage, thus avoiding dispute over chronology; on the other hand, the absolute age determination methods (such as thermoluminescence TL and U-series dating  $^{230}\text{Th}$ ) [28, 55] increase dating accuracy and enable the play of the advantage that loess has a high accumulation rate and can more easily record the geomagnetic events with a short timescale. However, for the strata in other periods of loess-paleosol sequences, this advantage is restricted in many aspects, such

as: the error of the accuracy of absolute age determination methods increases remarkably and the function of auxiliary dating is absent; the reliability of the horizon-time accuracy determined by astronomical timescale which is established through the comparison between magnetic susceptibility/grain size and oxygen isotope still needs verifying; the evaluation on the lock-in effect of loess remanent magnetization. Therefore, the ages of the short polarity events recorded in the loess stratum of late Matuyama and early Brunhes are often estimated by the method of interpolating the values between age control points on geomagnetic reversal boundaries [34,47,56]. No doubt, this alternate method makes the calculation easier, but before application, the reason for the anomaly of remanent magnetization recorded in stratal samples must be prudently evaluated.

Recently, Yang et al. [34] discovered two short polarity events in L9 at Baoji. As the age data they obtained are close to the Kamikatsura and Santa Rosa  $^{40}\text{Ar}/^{39}\text{Ar}$  ages, these events were confirmed as two excursions. However, the finding of the research made by Wang et al. [35] on L9 in Sha'anxian, Henan Province gives another view and thinks the normal polarity intervals in L9 is the remagnetization phenomenon controlled by lithology other than the record of geomagnetic excursion. Their bases are: (1) The whole section of the L9 in Sha'anxian except the thin layer in the middle part shows normal polarity, and the time corresponding to accumulation thickness doesn't tally with the duration of Kamikatsura and Santa Rosa; and (2) Sha'anxian is located in the highly active region of summer monsoon, the precipitation during S8 is profuse, and rainwater infiltration induces some low-coercivity magnetic grains in L9 to make rearrangement in the subsequent Brunhes chron and record the direction of present-day magnetic field. In view of this conclusion, while analyzing the possible causes of remagnetization, we also paid attention to the following facts: (1) Normal polarity interval is recorded in L9 at many areas of the CLP (such as Lanzhou, Xifeng, Luochuan, Baoji, Lantian, Weinan and Sanmenxia) [30–33,47], only the thickness or the position in the stratum that records this event is different. For example, in Lanzhou Jiuzhoutai, Baoji and Sanmenxia Songjiadian sections, this interval is in the middle part of L9; in Luochuan, Xifeng, Lantian and other sections, it is in the upper part or top; only in Sha'anxian, almost the whole section shows normal polarity. If we say that the precipitation during S8 is profuse, and rainwater infiltration induces the magnetic minerals among the coarse grains in L9 to make rotation and rearrangement in the subsequent Brunhes chron, it will be very difficult for us to explain why in Songjiadian, Baoji and Lanzhou Jiuzhoutai sections, this phenomenon did not happen at the top of L9 where soil solution is the most saturated and the corresponding grains are almost the coarsest in the whole section (Songjiadian section, Figure 5), it will be even more difficult for us to explain why remagnetization did not happen in the horizon between the two abnormal

segments of L9 in Songjiadian, where the grains are also very coarse and the texture is also loose. (2) Accumulation rate of loess may vary greatly with wind force, location, topography and dust source in different periods. (3) The record of Kamikatsura and Santa Rosa excursions has been discovered and researched in different lithofacies and localities all around the world [3,6,7,9,13,14,34,47], and the age data correspond to the depositional period of the loess in L9 (many researches have done on the formation and duration of L9. The time is concentrated in 865–952 ka B.P.) [39,57], so it is not impossible that loess unit L9 records the above short polarity events. Based on these analysis, we think it is more reasonable to explain the two magnetic anomalies in L9 of Songjiadian section with geomagnetic excursion.

SJD 1 and SJD 2 are completely recorded within the "upper sand layer" L9. L9 as a product of eolian dust deposits represents very dry and cold climatic period and corresponds to a desertic-semidesertic environment [58]. It shows exceptionally high dust sedimentation rates, very weak weathering [36] and large thickness. Recent research indicates the Lock-in effect to which weak weathered loess corresponds is not obvious [28] and the lock-in depth of NRM is small, too [59]. The thickness (11 m) of L9 in the Songjiadian section is even greater than that of L9 in other areas to its west, for example: Luochuan section (L9: 7.5 m in thickness) and Lingtai (L9: 10 m) [16] in central Loess Plateau, so the L9 of Songjiadian section is less influenced by CRM or the "Smoothing" effect of remanent magnetization caused by a low accumulation rate.

Based on the positions of UJ-M and M-B boundaries and boundary ages in this section [60], assuming a constant loess accumulation rate of 8.04 cm/ka between the UJ-M and M-B boundaries, midpoint ages of the short polarity events zones are estimated to be 0.917 Ma for the SJD 1, and 0.875 Ma for the SJD 2, respectively. The two short polarity events are separated by a fully reversed polarity zone spanning the stratigraphic interval between 45.15 and 46.10 m, with duration of 12 ka (Figure 7). If the chiloparts timescale of Ding [39] is used, this timescale assign ages of 0.865 Ma and 0.943 Ma to the S8/L9 and L9/S9-1 boundaries, respectively. Assuming a constant loess accumulation rate of 14.1 cm/ka between these two boundaries, midpoint ages for the two short polarity events zones are estimated at 0.930 Ma for the SJD 1, and 0.899 Ma for the SJD 2. The fully reversed polarity zone between the two short polarity events is estimated to span 7 ka with this age model. As different statistical methods are adopted, the two show a difference of about 0.013 Ma (SJD1, 0.917 vs 0.930 Ma) and 0.024 Ma (SJD2, 0.875 vs 0.899 Ma) in the estimation of the midpoint ages of short polarity events, but this does not affect the comparison between the above estimated data and the ages of the geomagnetic excursions recorded in the synchronous marine sediment and lava. Therefore, we believe 0.917 Ma and 0.875 Ma are good estimate values of

the midpoint ages of SJD 1 and SJD 2 short polarity events. In recent years, it has been discovered many times from marine sediment that the short polarity event of geomagnetic field occurred during 0.78–0.99 Ma [2–4]. The same is true of lava study. When Singer et al. [6,7] studied Cerro Santa Rosa I lava cone in 1999 and 2001, they gave 0.922–0.936 Ma—the dating result of Santa Rosa excursions. Many subsequent researches proved similar age data of this excursion [3,13]; Maenaka et al. gave 0.8 Ma—the age of Kamikatsura normal polarity event in 1983. In the later lava researches, the age data of this event was corrected to  $0.886 \pm 0.003$  Ma [6]. The latest ODP980-984 borehole data reveal that its age is 0.85 Ma [3,4] and suggest that Kamikatsura and Santa Rosa excursions correspond to the Marine Isotope Stage (MIS) 21 and MIS 25 top [13–15] (see Figure 8). As the chronological data of the above excursions are from different areas and different lithofacies strata, it indicates Kamikatsura and Santa Rosa excursions are global and universally recorded. As the estimated age (0.917 Ma) of SJD 1 obtained from this research is very close to the estimated age (0.922–0.936 Ma) of Santa Rosa excursion and the estimated age (0.875 Ma) of SJD2 is very close to the estimated age (0.85–0.899 Ma) of Kamikatsura excursion, SJD1 and SJD 2—the two short polarity events recorded in unit L9 of the Songjiadian section, in the Sanmenxia area should be the record of Santa Rosa and Kamikatsura excursions in terrestrial loess stratum.

## 5 Conclusions

The loess unit L9 of the Songjiadian section in the Sanmenxia area is developed with a high dust accumulation rate, less influenced by pedogenesis and experienced with no serious disturbance. By these advantages, it has clearly recorded two short polarity excursion events, the SJD 1 and

SJD. Using various age models, we obtained that the midpoint ages of the SJD 1 and SJD 2 events are 0.917 Ma and 0.875 Ma, respectively. The interval between the two event is about 12 ka. Based on the newly obtained paleogeomagnetic chronological data from deep ocean sediment and lava, the SJD 1 and SJD 2 detected in this study could be correlated respectively with the Santa Rosa and Kamikatsura geomagnetic excursions.

*We thank three anonymous reviewers for their critical review and thoughtful suggestions on the manuscript. This work was supported by the National Natural Science Foundation of China (Grant Nos. 40672114 and 40872112).*

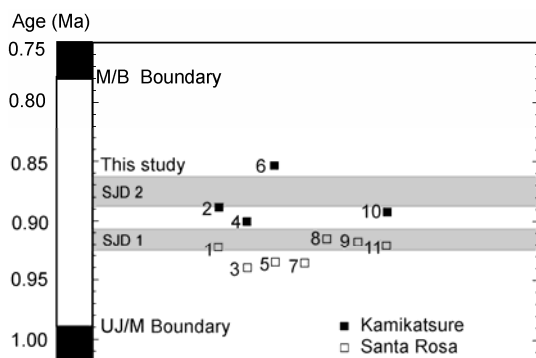


**Figure 8** Plots of ages for previously reported excursions in the late Matuyama Chron compared with those estimated in this study: 1,  $0.922 \pm 0.024$  Ma [6]; 2,  $0.886 \pm 0.003$  Ma [6]; 3,  $0.936 \pm 0.008$  Ma [7]; 4,  $0.899 \pm 0.006$  Ma [7]; 5, 0.932 Ma [3]; 6, 0.85 Ma [9]; 7, 0.932 Ma [13,14]; 8,  $0.915 \pm 0.008$  Ma; 9, 0.913 Ma [47]; 10, 0.89 Ma [34]; 11, 0.92 Ma [34]; polarity boundary ages are after Cande and Kent (1995) [60].

- Gubbins D. The distinction between geomagnetic excursions and reversals. *Geophys J Int*, 1999, 137: F1–F3 doi: 10.1046/j.1365-246x.1999.00810.x
- Channell J, Kleiven H F. Geomagnetic palaeointensities and astrochronological ages for the Matuyama-Brunhes boundary and the boundaries of the Jaramillo Subchron: palaeomagnetic and oxygen isotope records from ODP Site 983. *Philos Trans Roy Soc Lond*, 2000, 358: 1027–1047
- Channell J, Mazaud A, Sullivan P, et al. Geomagnetic excursions and paleointensities in the 0.9–2.15 Ma interval of the Matuyama Chron at ODP Site 983 and 984 (Iceland Basin). *J Geophys Res*, 2002, 107, doi: 10.1029/2001JB000491
- Channell J, Guyodo Y. The Matuyama Chronozone at ODP Site 982(Rockall Bank): Evidence for decimeter-scale magnetization lock-in depths. *AGU Geophysical Monograph Seminar*, 145: Time-scales of the Geomagnetic Field. Washington DC: 2004. 205–219
- Doell R R, Dalrymple G B. Geomagnetic polarity epochs: A new polarity event and the age of the Brunhes-Matuyama boundary. *Science*, 1966, 152: 1060–1061, doi: 10.1126/science.152.3725.1060
- Singer B S, Hoffman K A, Chauvin A, et al. Dating transitionally magnetized lavas of the late Matuyama Chron: Toward a new  $^{40}\text{Ar}/^{39}\text{Ar}$  timescale of reversals and events. *J Geophys Res*, 1999, 104: 679–693, doi: 10.1029/1998JB900016
- Singer B, Brown L L. The Santa Rosa event:  $^{40}\text{Ar}/^{39}\text{Ar}$  and paleomagnetic results from the Valles rhyolite near Jaramillo Creek, Jemez Mountains, New Mexico. *Earth Planet Sci Lett*, 2002, 197: 51–64, doi: 10.1016/0012-821X(01)00592-2
- Maenaka K. Magnetostratigraphic study of the Osaka group, with special reference to the existence of pre and post-Jaramillo episodes in the late Matuyama polarity Epoch. *Mem Hanazono Univ*, 1983, 14: 1–65
- Takatsugi K O, Hyodom. A geomagnetic excursion during the late Matuyama Chron, the Osaka group, southwest Japan. *Earth Planet Sci Lett*, 1995, 136: 511–524, doi: 10.1016/0012-821X(95)00175-1
- Singer B, Hildreth W, Vincze Y.  $^{40}\text{Ar}/^{39}\text{Ar}$  evidence for early deglaciation of the central Chilean Andes. *Geophys Res Lett*, 2000, 27: 1663–1666, doi: 10.1029/1999GL011065
- Coe R S, Singer B S, Pringle M S, et al. Matuyama-Brunhes reversal and Kamikatsura event on Maui: Paleomagnetic directions,  $^{40}\text{Ar}/^{39}\text{Ar}$  ages and implications. *Earth Planet Sci Lett*, 2004, 222: 667–684, doi: 10.1016/j.epsl.2004.03.003
- Quidelleur X, Carlut J, Gillot P Y, et al. Evolution of the geomagnetic field prior to the Matuyama-Brunhes transition: Radiometric dating of a 820ka excursion at La Palma. *Geophys J Int*, 2002, 151: F6–F10, doi: 10.1046/j.1365-246X.2002.01841.x
- Hong C S, Lee M Y, Pálíke H, et al. Astronomically calibrated ages for geomagnetic reversals within the Matuyama Chron. *Earth Planet Space*, 2002, 54: 679–690
- Hong C S, Roberts A P, Liang W T. Astronomically tuned record of

- relative geomagnetic paleointensity from the western Philippine Sea. *J Geophys Res*, 2003, 108: 2059, doi: 10.1029/2001JB001698
- 15 Channell J, Labs J, Raymo M E. The Réunion Subchronozone at ODP Site 981 (Feni Drift, North Atlantic). *Earth Planet Sci Lett*, 2003, 215: 1–12, doi: 10.1016/S0012-821X(03)00435-7
- 16 Liu T S. *Loess and the Environment*. Beijing: China Ocean Press, 1985.1–251
- 17 Zhou L P, Oldfield F, Wintle A G, et al. Partly pedogenic origin of magnetic variations in Chinese loess. *Nature*, 1990, 346: 737–739 doi: 10.1038/346737a0
- 18 Maher B A, Thompson R. Mineral magnetic record of the Chinese loess and Paleosol. *Geology*, 1991, 19: 3–6, doi: 10.1130/0091-7613(1991)019<0003: MMROTC>2.3.CO;2
- 19 Banerjee S K, Hunt C P, Liu X M. Separation of local signals from the regional paleomonsoon record of the Chinese Loess Plateau: a rock-magnetic approach. *Geophys Res Lett*, 1993, 20: 843–846, doi: 10.1029/1993/93GL00908
- 20 Florindo F, Zhu R X, Guo B, et al. Magnetic proxy climate results from the Duanjiapo loess section, southernmost extremity of the Chinese Loess Plateau. *J Geophys Res*, 1999, 104: 645–659, doi: 10.1029/1998JB900001
- 21 Heller F, Liu T S. Magnetostratigraphical dating of loess deposits in China. *Nature*, 1982, 300: 431–433, doi: 10.1038/300431a0
- 22 Zhu R X, Zhou L P, Laj C, et al. The Blake geomagnetic polarity episode recorded in Chinese loess. *Geophys Res Lett*, 1994, 21: 697–700, doi: 10.1029/94GL00532
- 23 Zhu R X, Laj C, Mazaud A. The Matuyama-Brunhes and upper Jaramillo transitions recorded in a loess section at Weinan, north-central China. *Earth Planet Sci Lett*, 1994, 125: 143–158, doi: 10.1016/0012-821X(94)90212-7
- 24 Zhu R X, Pan Y X, Guo B, et al. A recording phase lag between ocean and continent climate changes: constrained by the Matuyama/Brunhes polarity boundary. *Chinese Sci Bull*, 1998, 43: 1593–1598
- 25 Fang X M, Li J J, Van der Voo R, et al. A record of the Blake event during the last interglacial paleosol in the western loess plateau of China. *Earth Planet Sci Lett*, 1997, 146: 73–82, doi: 10.1016/S0012-821X(96)00222-1
- 26 Zhou L P, Shackleton N J, Dodonov A E. Stratigraphical interpretation of geomagnetic polarity boundaries in Eurasia loess. *Chinese Sci Bull*, 2000, 20: 196–202
- 27 Zhou L P, Shackleton N J. Misleading positions of geomagnetic reversal boundaries in Eurasian loess and implications for correlation between continental and marine sedimentary sequences. *Earth Planet Sci Lett*, 1999, 168: 117–130, doi: 10.1016/S0012-821X(99)00052-7
- 28 Zhu R X, Pan Y X, Liu Q S, et al. No apparent lock-in depth of the Laschamp geomagnetic excursion: Evidence from the Malan loess. *Chinese Sci Bull*, 2006, 49: 960–967, doi: 10.1007/s11430-006-0960-x
- 29 Zhu R X, Guo B. The reliability of secular variation of geomagnetic field of Lingtai profile in Gansu Province (in Chinese). *Sci China Ser D-Earth Sci*, 2000, 30: 324–330
- 30 Yue L P, Qu H J, Yang Y L, et al. Paleomagnetic Research of Loess Section from Jiuzhoutai, Lanzhou (in Chinese). *J Northwest Univ (Natural Science Edition)*, 1992, 22: 87–94
- 31 Yue L P. Palaeomagnetic polarity boundary were recorded in Chinese loess and red clay, and geological significance (in Chinese). *Chin J Geophys*, 1995, 38: 311–320
- 32 Zhu R X, Yue L P, Bai L X. Progress of Quaternary paleomagnetism in China (in Chinese). *Quat Sci*, 1995, 12: 162–173
- 33 Zhu R X, Tschu K K. *Studies on Paleomagnetism and Reversals of Geomagnetic Field in China*. Beijing: Science Press, 2001
- 34 Yang T S, Hyodo M, Yang Z Y, et al. Evidence for the kamikatsura and Santa Rosa excursions recorded in eolian deposits from the southern Chinese Loess Plateau. *J Geophys Res*, 2004, 109: B12105, doi: 10.1029/2004JB002966
- 35 Wang X S, Lovlie R, Yang Z Y, et al. Remagnetization of Quaternary eolian deposits: a case study from SE Chinese Loess Plateau. *Geochem Geophys Geosyst*, 2005, 6: Q06H18, doi: 10.1029/2004GC000901
- 36 Sun J M, Liu T S. Pedostratigraphic subdivision of the loess-paleosol sequences at Luochuan and a new interpretation on the paleoenvironmental significance of L9 and L15 (in Chinese). *Quat Sci*, 2002, 22: 406–412
- 37 Zhu R X, Liu Q S, Jackson M J. Paleoenvironmental significance of the magnetic fabrics in Chinese loess-paleosols since the last interglacial (<130 Ka). *Earth Planet Sci Lett*, 2004, 221: 55–69, doi: 10.1016/S0012-821X(04)00103-7
- 38 Hus J J. The magnetic fabric of some loess-paleosol deposits. *Phys Chem Earth*, 2003, 28: 689–699, doi: 10.1016/S1474-7065(03)00128-1
- 39 Ding Z L, Derbyshire E, Yang S L, et al. Stacked 2.6-Ma grain size record from the Chinese loess based on five sections and correlation with the deep-sea  $\delta^{18}\text{O}$  record. *Paleoceanography*, 2002, 17: 501–521, doi: 10.1029/2001PA000725
- 40 Pye K A. *Eolian Dust and Dust Deposits*. London: Academic Press, 1987. 1–265
- 41 Lu H Y, Zhang F Q, Liu X D, et al. Periodicities of palaeoclimatic variations recorded by loess-paleosol sequences in China. *Quat Sci Rev*, 2004, 23: 1891–1900, doi: 10.1016/j.quascirev.2004.06.005
- 42 Rutter N W, Ding Z L, Evans M E, et al. Magnetostratigraphy of the Baoji loess-paleosol section in the north-central China Loess Plateau. *Quat Int*, 1990, 7: 97–102, doi: 10.1016/1040-6182(90)90043-4
- 43 Guyodo Y, Richter C, Valet J P. Paleointensity record from Pleistocene sediments (1.4–0 Ma) of the California Margin. *J Geophys Res*, 1999, 104: 2953–2964, doi: 10.1029/1999JB900163
- 44 Kok Y S, Tauxe L. A relative paleointensity stack from Ontong-Java Plateau sediments for the Matuyama. *J Geophys Res*, 1999, 104: 25401–25413, doi: 10.1029/1999JB900186
- 45 Zhu R X, Laj C, Mazaud A. The Matuyama-Brunhes and Upper Jaramillo transitions recorded in a loess section at Weinan, north-central China. *Earth Planet Sci Lett*, 1994, 125: 143–158, doi: 10.1016/0012-821X(94)90212-7
- 46 McIntosh G, Rolph T C, Shaw J, et al. A detailed record of a normal-reversed-polarity transition obtained from a thick loess sequence at Jiuzhoutai, near Lanzhou, China. *Geophys J Int*, 1996, 127: 651–664, doi: 10.1111/j.1365-246X.1996.tb04045.x
- 47 Pan Y X, Zhu R X, Liu Q S, et al. Geomagnetic episodes of the last 1.2 Myr recorded in Chinese loess. *Geophys Res Lett*, 2002, 29: 1282, doi: 10.1029/2001GL014024
- 48 Ge S L, Shi X F, Zhang W B. General review for methods of relative geomagnetic paleointensity (in Chinese). *Mar Geol Quat Geol*, 2007, 27: 65–70
- 49 Yang T S, Hyodo M, Yang Z Y, et al. Two geomagnetic excursions during the Brunhes chron recorded in Chinese loess-paleosol sediments. *Geophys J Int*, 2007, 171: 104–114, doi: 10.1111/j.1365-246X.2007.03522.x
- 50 Yang T S, Hyodo M, Yang Z Y, et al. Early and middle Matuyama geomagnetic excursions recorded in the Chinese loess-paleosol sediments. *Earth Planet Space*, 2007, 59: 825–840
- 51 Zhu R X, Pan Y X, Liu Q S. Geomagnetic excursions recorded in Chinese loess in the last 70, 000 years. *Geophys Res Lett*, 1999, 26: 505–508, doi: 10.1029/1999GL900019
- 52 Zheng H, Rolph T, Shaw J, et al. A detailed palaeomagnetic record for the Last Interglacial period. *Earth Planet Sci Lett*, 1995, 133: 339–351, doi: 10.1016/0012-821X(95)00089-U
- 53 Zheng H, An Z, Shaw J. New contribution to Chinese Pliocene-Pleistocene magnetostratigraphy. *Phys Earth Planet Inter*, 1992, 70: 146–153, doi: 10.1016/0031-9201(92)90177-W
- 54 Heslop D, Shaw J, Bloemendal J, et al. Sub-millennial scale variations in east Asian monsoon systems recorded by dust deposits from the north-western Chinese Loess Plateau. *Phys Earth Planet Inter (A)*, 1999, 24: 785–792, doi: 10.1016/S1464-1895(99)00115-5
- 55 Wang Y J, Cheng H, Edwards R L, et al. A high-resolution absolute-dated Late Pleistocene monsoon record from Hulu Cave,

- China. *Science*, 2001, 294: 2345, doi: 10.1126/science.1064618
- 56 Zhu R X, Potts R, Xie F, et al. New evidence on the earliest human presence at high northern latitudes in northeast Asia. *Nature*, 2004, 431: 559–562, doi: 10.1038/nature02829
- 57 Heslop D, Langereis C G, Dekkers M J. A new astronomical timescale for the loess deposits of Northern China. *Earth Planet Sci Lett*, 2000, 184: 125–139, doi: 10.1016/S0012-821X(00)00324-1
- 58 Guo Z T, Liu T S, Fedoroff N, et al. Climate extremes in Loess of China coupled with the strength of deep-water formation in the North Atlantic. *Glob Planet Change*, 1998, 18: 113–128, doi: 10.1016/S0921-8181(98)00010-1
- 59 Yang T S, Li H D, Fu J L, et al. Investigation on the Lock-in depth of paleosol S7 and loess L8 in Baoji (in Chinese). *Quat Sci*, 2007, 7: 972–982
- 60 Cande S C, Kent D V. Revised Calibration of the geomagnetic polarity timescale for the Late Cretaceous and Cenozoic. *J Geophys Res*, 1995, 100: 6093–6095, doi: 10.1029/94JB03098